

## Research Article

# Intelligent UAV Map Generation and Discrete Path Planning for Search and Rescue Operations

Víctor San Juan,<sup>1</sup> Matilde Santos ,<sup>1</sup> and José Manuel Andújar <sup>2</sup>

<sup>1</sup>Department of Computer Architecture and Automatic Control, Faculty of Informatics, University Complutense of Madrid, 28040 Madrid, Spain

<sup>2</sup>Department of Electronic, Computer Science and Automatic Engineering, University of Huelva, 21819 Huelva, Spain

Correspondence should be addressed to Matilde Santos; msantos@ucm.es

Received 9 December 2017; Accepted 28 February 2018; Published 23 April 2018

Academic Editor: Dimitri Volchenkov

Copyright © 2018 Víctor San Juan et al. This is an open access article distributed under the Creative Commons Attribution License, which permits unrestricted use, distribution, and reproduction in any medium, provided the original work is properly cited.

Search and Rescue Operations (SAR) take place in any emergency situation where people are involved and their lives are at risk. These operations are nowadays carried out with the help of advanced technology, such as Unmanned Aerial Vehicles (UAVs). In this work, several methods are proposed to calculate the UAV discrete path planning. Previously, an intelligent characterization of the searching area is performed to estimate a potential risk/occupancy degree of the gridding map. This estimation is mainly based on fuzzy logic, considering different factors. Then, four methods are applied to calculate the path planning: an original proposal called attraction, fuzzy logic, ANFIS, and a PSO algorithm. All of them calculate the location of the waypoints to be followed by the UAVs to minimize the distance and the risk the people is exposed to. Then, these strategies are adapted to the possibility of having more than one UAV searching at the same time, and the swarm formation is discussed. Finally, these four solutions for path planning, including different number of UAVs, are tested in a real simulation scenario, and then the performance of each method is analyzed and compared with the others.

## 1. Introduction

Unfortunately, every year there are some news of natural disasters, like fires or earthquakes which affect cities, towns, and natural environment. Besides, we also see human tragedies as maritime accidents or people who get lost in hazardous places. All these situations, and many others, have one important aspect in common. They subject the life of many people involved in these situations in one way or another to danger and a direct risk.

The most critical aspect in these cases, even before starting to mitigate the risk (i.e., extinguishing a fire), is the search and rescue (SAR) of potential survivors. The SAR process is carried out by specialized teams that even risk their own lives to save others.

Fortunately, these SAR teams are, in most of the cases, well equipped with advanced technology, which nowadays includes Unmanned Aerial Vehicles (UAVs) to improve people searching and also to prevent rescue team from

going through risky places with no real evidences of finding survivors [1].

These autonomous vehicles have experienced a huge development during the last ten years. UAVs are nowadays used in many different applications such as defence, surveillance, or package delivery, among others [2]. But the unmanned aerial vehicle path planning problem is an important issue in the UAV mission planning [3].

Many of these applications use automatically controlled aerial vehicles, which are able to flight through a preplanned trajectory or even to make a real-time decision on the trajectories. Nevertheless, most of the commercial UAVs still use an off-board pilot and a fixed preplanned trajectory [4].

The final motivation of this work is to find people at risk as fast as possible in SAR operations, using fully automatic UAVs equipped with on-board cameras. Therefore, we proposed some strategies to optimize this searching. The path planning takes into account the hazard of a particular scenario, where there will be some places with higher risk

than others. To do this, we have first developed a methodology based on fuzzy logic to characterize the surface to be explored and to estimate the degree of potential risk and the probability of people to be at that spot.

Then, we have developed a discrete path planner to find people as fast as possible using the map generated by the previous analysis. Four intelligent discrete path planning strategies have been implemented and tested on a real scenario. Finally, we will show how the number of UAVs in swarm formation affects the speed and effectiveness of people searching.

The following topics are not included in the scope of this work: UAV on-board control and obstacle avoidance and UAV path following and image processing. In fact, we are not working with a model of the dynamics of the UAV. The path planning is calculated as a trajectory along some discrete points, corresponding to different cells in which the map of the searching area is divided. The UAV moves from one cell to another (the adjacent one) with a constant speed. The number of cells visited gives the length of the trajectory and therefore the time spent.

The paper is organized as follows: Section 2 summarizes the related works. Section 3 describes the generation of the fuzzy occupancy/risk map. In Section 4, four approaches for the intelligent discrete path planning are proposed and results on a real simulation scenario are presented and analyzed. The outcome of using several UAVs in the search and rescue mission is discussed in Section 5. Section 6 shows a case studied and Section 7 summarizes and discusses the global results. The paper ends with the conclusions and future work.

## 2. Background

Search and Rescue (SAR) operations must be carried out by the competent authorities in case of emergency that involves people in danger. The nature of these emergencies can be very different; therefore, the hazards will vary depending on the kind of emergency and consequently the SAR mission has also to be adapted to the scenario. Some emergency situations are, for instance, people lost in uninhabitable places, fires, aircraft or vessel accidents, natural disasters like landslides, floods, and earthquakes [5].

Autonomous robots and vehicles have been used to carry out missions in hazardous environments, such as operations in nuclear power plants, exploration of Mars, and surveillance of enemy forces in the battle field [6]. Indeed, UAVs are often used in SAR operations. The common operation of these UAVs is to be commanded remotely by a SAR team member [7]. The UAV is moved by its pilot to the desired areas in order to collect the relevant information for the SAR mission [8]. The payload of the UAV may be of different nature, usually cameras to record video or to take pictures, but it is also possible to find other sensors such as gas analyzers to detect smoke composition.

But still planning a SAR mission in terms of obtaining the path or trajectory is a challenging issue that requires careful consideration. The autonomous UAVs flight can be based on a preplanned path or can even be calculated online [9]. The level of autonomy achieved by the UAVs depends on

the methodology used to control the vehicle and to generate its routes [10]. Therefore, autonomous UAVs must have an auto path planning calculation functionality to be really autonomous.

Discrete search is an interesting topic nowadays, with many applications. For example, in built infrastructure monitoring, an efficient path planning algorithm is essential for robotic inspection of large surfaces using computer vision [11, 12] or for controlling autonomous agents in interactive virtual worlds, given the growing demands on the size and complexity of these virtual scenarios, even for areas of crowd animation and whole-body motion planning for virtual characters [13].

Discrete path planning has different approaches. The book by Kallmann and Kapadia [13] reviews the evolution of several related techniques for achieving intelligent navigation in discrete spaces, starting from classical planning and computational geometry techniques and then gradually moving towards more advanced topics, although being applied to interactive virtual worlds, to address shortest paths and limited time budgets. Some of the path following algorithms more often used for UAVs are presented in [14], including a comparison between them in order to help in the selection of one or another. Geometrical methods such as spline interpolation are used in order to get smoother curves through a number of waypoints [15, 16]. In [7], path planning is defined using a Monte Carlo searching of the best path using online detected parameters.

The optimization of the path between waypoints is also addressed by several authors. Many of them use genetic algorithms (GA) [17–20]. Other proposals apply estimation of distribution algorithms [21] or  $A^*$  searching [22]. Generally, in these cases, the UAV needs to move in a known environment, and the optimal path is obtained to avoid obstacles, radar zones, buildings, battery run out, and so on.

## 3. Generation of the Risk/Occupancy Map

In this process of searching and rescue, it is desirable to exploit the increasing availability of data about a disaster that come from different sources. In particular, such information can be a valuable resource to drive the planning of UAV flight paths over a space in order to discover people who are in danger [8]. Therefore, the first step will be to estimate and define the searching area, including all the available data, and define the desired area coverage level, in order to generate the map that will be used for the discrete UAVs path planning.

This area characterization involves the analysis of the surface where the search will take place and the quantification of some characteristics. The input is a map of the area to be covered. This map is divided into a grid of cells. Each of these cells will have an assigned value of potential risk and occupancy that will be used to calculate the waypoints that the UAV will follow.

To make the grid partition, it is assumed that the UAV will be able to track the whole cell when located at the geometrical centre of it. That is, the size of the cells will not be bigger than the area covered by the on-board camera of the UAV. But this is difficult to be estimated since it depends on two

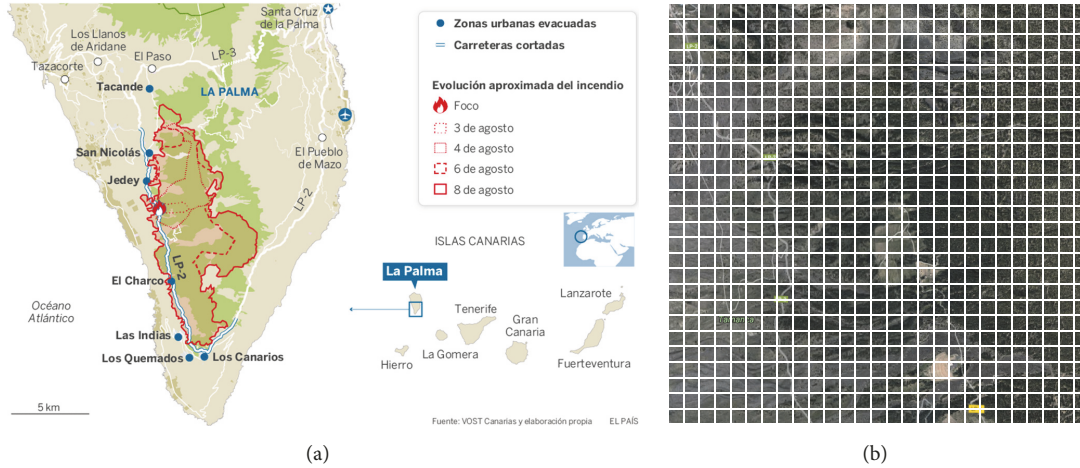


FIGURE 1: La Palma fire map (a) and gridding searching area (b).

main factors: the altitude of the UAV and the opening angle of the camera lens. At the same time, the altitude of the UAV, in case of visual tracking, will be limited for the camera characteristics. In fact, if the altitude is too high, the camera will not be able to focus correctly, and therefore the tracking will not work. Taking this into account and considering that we are working with a discrete scenario in a theoretical way, a limit of  $100 \times 100$  m cell size has been established. This value can be scaled according to the technical specifications of the sensors used.

Once the size of the grid is determined, the number of cells is calculated straightforward for the particular zone we are exploring.

The application scenario of this work is a real case. In August 2016, a forest fire was declared in the island of La Palma, in the Canary Islands (Spain). The fire lasted several days affecting over 4000 hectares, that is, 6.8% of the island surface (Figure 1(a)). Fortunately, there were no civil victims, but sadly one person died during the extinguishing phase. More than 2500 people needed to be evacuated from their homes during the fire.

In Figure 1(a), we can see how the fire grew throughout the days. The simulation scenario corresponds to the third day of the fire (dotted red line). Three days is a reasonable time to search for a person. A rectangular area, larger than the fire area, was selected to be tracked and partitioned. The grid partition has  $24 \times 24$  cells (Figure 1(b)).

Once the region to be covered is defined and the grid partition obtained, the potential risk/occupancy value for each cell is going to be estimated.

**3.1. Potential Risk/Occupancy Estimation.** The potential risk/occupancy map aims to give a value of the possibility of each cell to be occupied by people and, in that case, the potential hazard for the life of that person.

To calculate this value some information from different sources is necessary. To obtain the potential occupancy we need to know, for example, how often the area is visited by people. The potential risk can be given by the types

of emergencies. This information can be obtained from an analysis of the area by experts and/or from historical data. We will consider two main components to define the map, called terrain and emergency factors. They are defined by fuzzy inference systems (FIS).

The terrain FIS has as inputs the variables named *staying*, *hazard*, and *transit* (Table 1). The output is *Pterrain*, which is the contribution of this factor to the map.

Two of these input variables have been defined as fuzzy (*staying* and *hazard*), and the third one (*transit*) will be considered as a crisp weight to be applied to the output. Both the *staying* and the *hazard* linguistic variables are normalized between 0 and 1. The fuzzy sets are given by triangular and trapezoidal membership functions. The labels are Low, Mid, and High for *staying* (Figure 2(a)) and Low and High for *hazard* (Figure 2(b)).

The output is defined by three triangular fuzzy sets (Low, Mid, and High). The fuzzy rules, obtained by applying expert knowledge, are as follows:

Rule	Staying	Hazard	Output
1	high	high	high
2	high	low	low
3	medium	high	high
4	medium	low	medium
5	low	high	medium
6	low	low	low

The output of this fuzzy system is finally weighted by the *transit* variable. That is, the terrain FIS result is multiplied by it to obtain the final *Pterrain* value. The *transit* variable will be low, in general, in places where the access is easy and it is difficult that people get lost and stay there (low occupancy); if something happened, they will have been already found and evacuated. Besides, the risk will be also low as there will be help to solve that situation. Therefore, the transit value will lower the value of *Pterrain* in this case. And vice versa.

This *Pterrain* factor is part of the contribution to the final value that will be assigned to each cell in order to rank them to be visited (see equation (1)).

TABLE I: Terrain factor inputs.

Staying	It describes whether the area is often visited by people or not. High values increase potential occupancy. This information can be obtained from an analysis of the area and/or from historical data.
Hazard	It quantifies the hazards inherent to the area, affected by wild animals, weather conditions, terrain access, etc. Higher values increase potential risk.
Transit	It expresses whether the area is usually transited by people, meaning people could be more easily found by other people. The potential occupancy and the risk of these areas decrease.

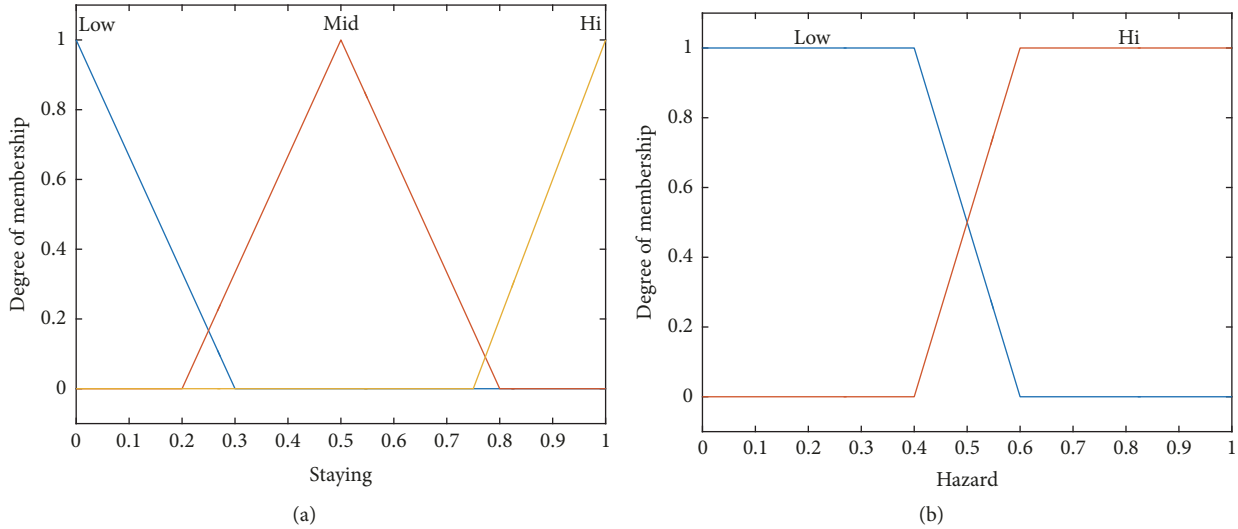
FIGURE 2: *Staying* (a) and *hazard* (b) fuzzy variables.

Table 3 shows an example of the values that these variables may have. The values given to the *staying* factor are estimated according to the terrain accessibility and orography. Inaccessible areas or areas with difficult access have smaller staying factor than others like roads or plains. The *hazard* has been estimated according to the terrain nature as well. The transit value depends on the presence of roads or buildings on that area.

To give an example, if the staying input is high, the contribution of the terrain factor to the risk/occupancy value of a cell should be high (there will be people there) but at the same time this value will be balanced for two other factors, transit and hazard. Anyway, if the staying is high it is very likely that the hazard of that place is low (no dangers) and in addition the transit factor will be low (roads, accessible places), decreasing the final contribution to the risk.

The same reasoning has been applied to determine the emergency FIS. The fuzzy input variables are *affected* and *injuries*, where *affected* is defined by three fuzzy sets with triangular membership functions and *injuries* has two trapezoidal ones. The third input, the *SAR team position*, is a binary variable with value equal to one except in the case the rescue team is already on the spot, in which case is 0. The definition of these variables is shown in Table 2. The output of this FIS is called *Pemergency* (see equation (1)).

For example, if a particular zone is strongly affected, and the type of accidents is dangerous for people lives, the value

of this FIS will be high. It will be pondered by whether the SAR team is near or even already there, decreasing the risk and the occupancy.

Finally, regarding the importance of *Pterrain* and *Pemergency* factors on the final decision about the path planning, the meaning of them is as follows. The first one is more important since it represents the zones that have to be visited because is very likely that people are there. Besides, they can also be hazardous areas. However, *Pemergency* represents the zones that should be visited because they are potentially dangerous for people due to some kind of emergency, in case people are there.

**3.2. Potential Risk/Occupancy Map.** We estimate the result of these fuzzy inference systems, *Terrain* and *Emergency*, for each cell of the map of the searching area of La Palma. A map is generated for both of them (Figure 3).

The colour represents the value of the corresponding factor for that cell, from dark blue (value 0) to yellow (value 1). Figure 3(a) shows the terrain contribution. A high staying factor can be observed in the middle of the map, and the secondary roads are clearly marked in blue. The emergency contribution is shown in Figure 3(b). There are three differentiated zones: the not affected one, the one in the middle that has been seriously affected by the fire and a pale green one.

TABLE 2: Emergency factor inputs.

Affected	It represents how the area is affected by an emergency. High values increase potential risk and low values the opposite.
Injuries	It describes the possibility of people being injured. High values increase potential risk.
SAR team position	It describes the location of the SAR team, e.g., how close to the emergency area they are. Indeed if the spot is already covered, the necessity of going to that point is cancelled.

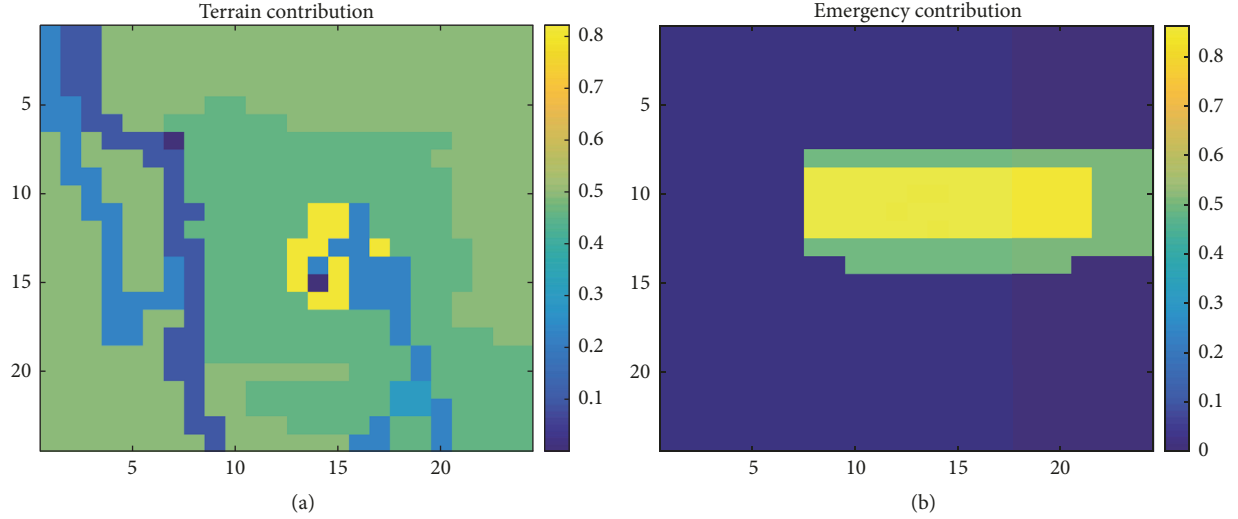


FIGURE 3: La Palma terrain (a) and emergency (b) maps.

TABLE 3: Terrain input values.

Description	<i>Transit</i>	<i>Staying</i>	<i>Hazard</i>
Main roads	0.2	0.8	0.1
Sec roads 1	0.4	0.6	0.2
Sec roads 2	0.6	0.4	0.2
Forest nearby	0.4	0.4	0.3
Plain	0.3	0.7	0.2
Forest type 1	0.6	0.4	0.4
Forest type 2	0.8	0.3	0.5
Forest type 3	0.9	0.1	0.7
Hills	0.5	0.5	0.3
Desert	0.9	0.2	0.6

Then both contributions are combined according to the relation given by (1) to obtain the potential risk/occupancy value of the zone caught on fire of La Palma (Figure 4), which will be the input for the discrete path planning:

$$P = 0.5 \cdot P_{\text{TERRAIN}} + 0.4 \cdot P_{\text{EMERGENCY}} + 0.1 \cdot P_{\text{HISTORICAL}} \quad (1)$$

The third term of (1), the historical contribution, quantifies the possibility of an event to happen again in the same place. It will be 1 in the positive case and 0 otherwise.

It is possible to see the different elements of the area; for example, some roads can be clearly identified and the yellow

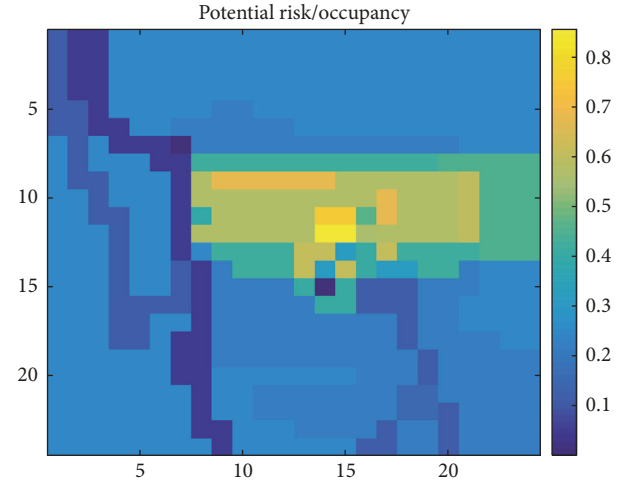


FIGURE 4: La Palma potential risk/occupancy map.

areas correspond to the forest, with higher risk values and where the fire started.

#### 4. Discrete Path Planning

Four approaches for discrete path planning have been develop and applied, three of them using techniques that come from the artificial intelligence field. The final aim is to define the waypoints the UAV must follow, in order to find

as quickly as possible the people involved in a SAR operation and to minimize the risk of their lives.

To find people in the fastest way, it is necessary to explore the whole area minimizing the travelled distance. Moreover, not only the time but also the risk has to be minimized, so the UAVs should first go to those zones which are riskier or more hazardous. As it is difficult to solve both problems at the same time, firstly the areas with higher potential risk/occupancy will be visited and then the distance will be minimized as well, looking for a good trade-off between both aims.

As it has been said, the on-board camera is supposed to be able to track a whole cell of the grid partition and the waypoints will be located at the centre of these cells. The path planning consists then in setting the order the cells should be gone through.

To check the quality of the solution, the results are quantified by two figures:

- (i) Distance ( $d$ ) is the total distance travelled by the UAV.
- (ii) Weight ( $w$ ) is a factor that is calculated as

$$w = \sum_i^n \sum_j^m \text{order}(i, j) \cdot P(i, j), \quad (2)$$

where order is the correlative position of the cell ( $i, j$ ) that is tracked and  $P$  is the potential risk/occupancy value of that cell. The meaning of this weight value is to quantify whether the most important cells, those with high  $P$  values, are tracked earlier than the other ones, so it is interesting to minimize it.

The scenario for the four approaches is the  $24 \times 24$  cell map shown in Figure 4 that corresponds to the fire affected area in La Palma.

**4.1. First Proposal: Attraction Approach.** This so-called *attraction approach* is based on the potential fields' theory. In general, potential fields are used when the final point is known. A vector is calculated and its direction and magnitude depend on the distance to this final point, taking into account the obstacles or forbidden zones that could affect the trajectory.

In our case, the final point is unknown. To define it, an attraction value is estimated for each cell so that the cell with the highest attraction value will be the next waypoint. The attraction value depends directly on the potential risk/occupancy of the cell and the distance to the current position (3). In this expression (3),  $A(i, j)$  represents the  $ij$ th cell of the attraction matrix  $A$  and  $P(i, j)$  the potential risk/occupancy associated with that cell. Covered matrix contains the historical information about whether the cell has been already tracked. That is, covered is a matrix with the same dimension as  $P$  and  $A$ , with value 1 for nontracked cells and 0 for traced ones. The denominator is the Euclidean distance from the  $ij$ th cell to the current position

$$A(i, j) = \frac{P(i, j) \cdot \text{Covered}(i, j)}{\sqrt{(x_{ij} - x)^2 + (y_{ij} - y)^2}}. \quad (3)$$

The algorithm tries to go to the points with high  $P$  values but near the current position, so further cells with high

$P$  values have less attraction than nearer points. Therefore, the trajectory is consistent and the UAV tracks low and high  $P$  cells minimizing the distance, but always being more attracted by higher  $P$  cells. If the distance was not taken into account, only  $P$  values would decide the waypoints, so the trajectory could have jumps from one waypoint to another and it may be bumpy.

Nevertheless, according to this proposal, the attraction by the distance is bigger than by the potential risk/occupancy value. So, in fact, the trajectory tries to first minimize the distance and then the potential risk/occupancy. While minimizing the distance is interesting, to minimize the weight is even more important because it is crucial to go first to the cells where the probability of finding someone is higher. Thus, (3) is changed to (4) in order to have a more balanced relation between those factors:

$$A(i, j) = \frac{P(i, j) \cdot \text{Covered}(i, j)}{\exp\left[\sqrt{(x_{ij} - x)^2 + (y_{ij} - y)^2}\right]}. \quad (4)$$

In (4), the exponential function of the distance has been chosen because of its asymptotic behaviour. The very close cells will take advantage of the distance, but in a short term all the cells will be similarly affected, in opposition to previous linear relationship, where further cells had less chance to be explored than nearer ones.

Two more improvements are made in order to get a better solution. The first one is about the continuity of the trajectory. To avoid jumps between consecutive cells a sequence of conditional rules is implemented. According to this, if two consecutive waypoints are located on the same vertical or horizontal line, all cells between these two points become automatically waypoints. This way these cells are considered already tracked and the UAV will not have to go backwards to explore them.

The second enhancement of the algorithm is about the waypoint selection. The cell with the maximum attraction is chosen as waypoint, but sometimes more than one cell has the same maximum value. Initially the first maximum found was selected, so the path depended on the starting point. A control strategy has been applied to avoid this bias. The first waypoint will be the cell that, having the maximum attraction value, is surrounded by cells with higher  $P$  values than the other candidates; that is, it is located in areas with more  $P$  density. A matrix with this density,  $Pg$ , is generated, according to the following formula:

$$Pg(i, j) = \sum_{n=i-2}^{i+2} \sum_{m=j-2}^{j+2} \frac{P(m, n)}{\sqrt{(x_{ij} - x_{nm})^2 + (y_{ij} - y_{nm})^2}}, \quad (5)$$

$\forall n \neq i, m \neq j.$

Then, after finding the maximum values of attraction of matrix  $A$  (4), a searching for the maximum  $Pg$  values (5) is carried out. The cell with highest density among the maximum attractions cells is selected as the next waypoint.

With all these modifications, a simulation is run on La Palma map to show this approach (Figure 5).

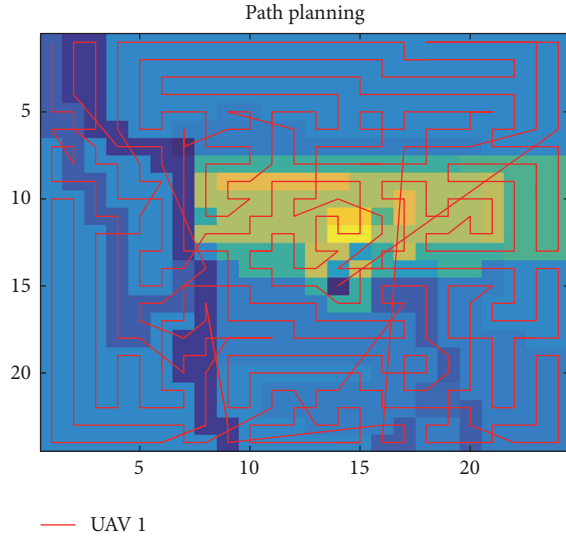


FIGURE 5: La Palma attraction path planning.

The trajectory starts at the top left corner and covers the entire surface. It seems to be consistent, with good continuity. The value of the distance is 680 units and the weight is 37392. As expected, the trajectory starts going across the light blue cells to the green ones, to quickly cover the yellow part of the map (higher  $P$  values). When the UAV gets near yellow cells, it goes directly to it and then covers all the nearer low  $P$  cells, without wasting time exploring low  $P$  cells that are automatically considered visited. Then it goes to the other yellow zones and so on.

To summarize, this original proposal works well and it is quite simple, but still the behaviour could be improved because there are some loops and paths cross each other. Other strategies will be tested.

**4.2. Fuzzy Logic Approach.** A different approach using fuzzy logic has been also implemented. A Mamdani Fuzzy Inference System (FIS) is designed with two inputs,  $P$  (potential risk/occupancy) and  $d$  (distance), and one output, attraction matrix ( $A$ ). This way the contribution of the potential risk/occupancy value and the distance to the current position are separated and a nonlinear relationship between them is generated. For each input, three triangular and trapezoidal fuzzy sets have been assigned (high, medium, and low) and two for the output (high and low). The nine fuzzy rules are given in Table 4.

Simulations were carried out on different scenarios to test this initial fuzzy approach. The results were worse than with the previous solution. When analyzing the evolution of the trajectory, we found that the UAV prefers to go to an adjacent cell with a lower  $P$  value instead of going to further cells with high  $P$  values. In fact, the yellow cells are first surrounded by the UAV but not tracked until later.

Although a FIS is usually designed and adjusted by an expert who knows the behaviour of the system, in this case the knowledge was quite poor. So, as the target is to minimize distance and risk, an optimization method can be used to tune

TABLE 4: Rules of the fuzzy approach.

Rule	$P$	$D$	$A$
1	High	High	High
2	Medium	High	Low
3	Low	High	Low
4	High	Medium	High
5	Medium	Medium	Low
6	Low	Medium	Low
7	High	Low	High
8	Medium	Low	High
9	Low	Low	High

TABLE 5: GA parameters.

Generations	300
Initial population	200
Stall generations limit	100
Average relative change limit (TolFun)	$10^{-10}$
Crossover fraction	0.8
Mutation distribution	Gaussian, scale, and shrink equal to 1

the membership functions. That is, an evolutionary FIS is implemented, which consists of the same FIS proposed above but adjusted with genetic algorithms.

The configuration of the GA must include the 32 parameters of the trapezoidal membership functions of the FIS. Each trapezoidal membership function is defined by 4 points:  $x_1$ ,  $x_2$ ,  $x_3$ , and  $x_4$ . The value of these parameters must be correlative; that is,  $x_1$  must be smaller than  $x_2$ ,  $x_2$  than  $x_3$ , and so on. These restrictions are defined by the linear constraints  $Ax < b$ , being  $b = 0.001$  in our case.

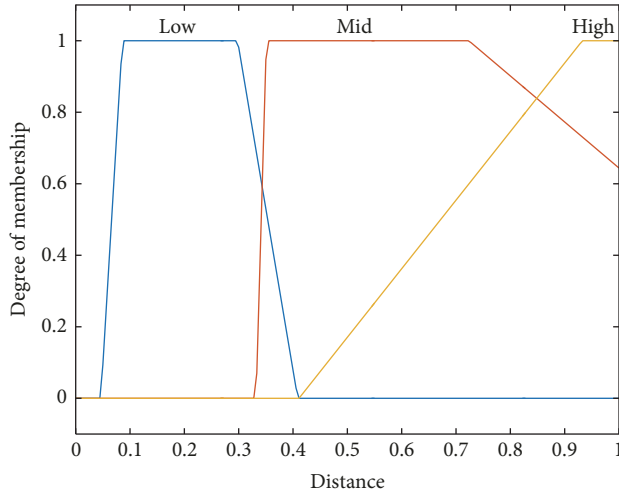
The fitness criterion is a function of the weight and the distance, both normalized in the range  $[0, 1]$  and to be minimized as follows:

$$f = \left[ 1 - \frac{\sum_{i=1}^{\max(i)} \sum_{j=1}^{\max(j)} P(i, j)}{w} \right] + \left[ 1 - \frac{\max(i) \cdot \max(j)}{d} \right]. \quad (6)$$

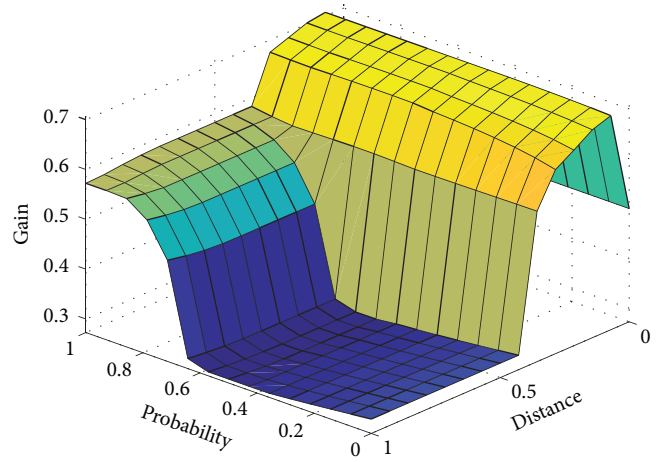
The rest of the GA parameters are shown in Table 5.

Initially, the process was so computationally slow that makes the problem unaffordable for this work. In order to reduce the computational time, we consider a smaller  $P$  map, and once the membership functions have been adjusted, it is scaled to a bigger one to see how it fits. Therefore, the GA is executed with the same configuration described but for a  $5 \times 5$   $P$  matrix.

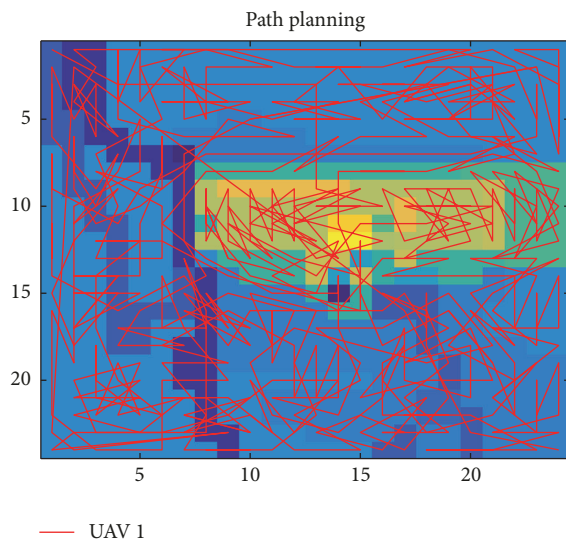
As an example, Figure 6 shows the membership functions of the input variable distance (a) and the output surface (b) after the GA adjustment. In the surface it is possible to see high output values for short distances and also for high  $P$  values in long distances.



(a)



(b)

FIGURE 6: Membership function of input *distance* (a) and fuzzy output *surface* (b).

— UAV 1

FIGURE 7: La Palma fuzzy logic path planning.

A test is now carried out with the  $25 \times 25$   $P$  map of La Palma (Figure 7), using the membership functions calculated for the  $5 \times 5$  map.

The results are  $d = 1497$  and  $w = 35951$ . Although the distance is much longer than in the attraction solution, weight is lower. Therefore we can say this solution also meets the target but with a stronger tendency to minimize risk/occupancy versus distance. However, the small angles that represent the transitions between two consecutive waypoints are not realistic and make the trajectory unaffordable for a UAV.

The strength of this approach is the fast convergence to the high  $P$  value cells, visiting later the lower  $P$  cells. This means that, even covering all the cells in a longer time, since the weight is lower and it also quantifies the occupancy, the probability of finding people in a short time is higher.

**4.3. ANFIS Approach.** Another solution is implemented using an Adaptive-Neuro-based Fuzzy Inference System (ANFIS) [23]. The FIS is the same as the previous one but the membership functions are now modified by the ANFIS algorithm.

Besides, a new input variable is included, the density matrix  $Pg$  (5). Now the system is able to give higher attraction values to higher density areas, instead of only using this factor for the selection of the maximum.

Therefore, the inputs are  $P$ ,  $d$ , and  $Pg$ . The first two are normalized and the range of  $Pg$  is  $[0.5, 5]$ . Three Gaussian membership functions are calculated for each variable. The output is again attraction matrix  $A$ . But ANFIS requires samples for training. Hence, we have generated 80 synthetic data sets manually. The training is performed during 50 epochs (Figure 8(a)). An example of the membership functions generated for the new variable  $Pg$  is shown in Figure 8(b).

The new generated control surfaces are shown in Figure 9. It is possible to observe the difference with the one shown in Figure 6(b). In this case they are smoother although clearly nonlinear.

Once the ANFIS has been generated, simulations are run on the real scenario of La Palma. The trajectory is shown in Figure 10. The results obtained are  $d = 808$  and  $w = 36284$ .

In this case, compared with the fuzzy logic solution ( $d = 1497$  and  $w = 35951$ ), the weight is higher but distance is much shorter, so it is not so easy to say which is better. However, what is really interesting of this approach is how the UAV goes over the highest  $P$  cells first, finishing the searching on low  $P$  cells.

**4.4. Using Particle Swarm Optimization (PSO).** Although the previous solutions seem to meet the main goal, they can be improved. In this case, an evolutive approach, a Particle Swarm Optimization (PSO) based solution is now proposed.

The GA was used to obtain the order of the cells that should be visited. GA worked well in small size maps but,

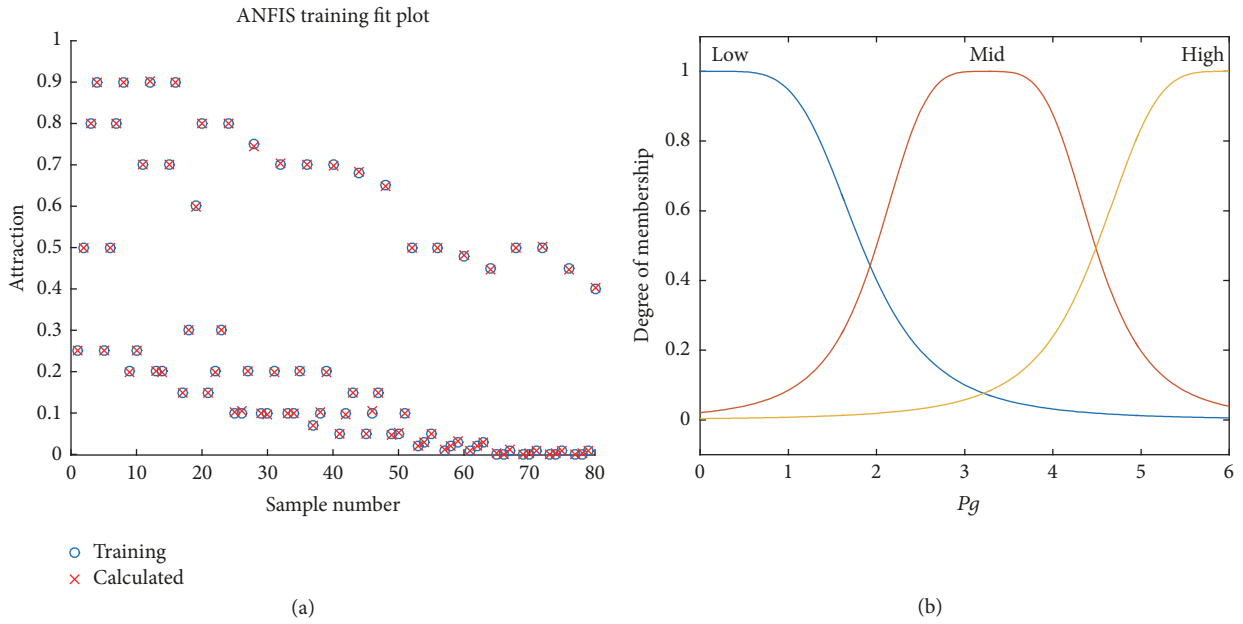


FIGURE 8: ANFIS training (a) and  $Pg$  membership functions (b).

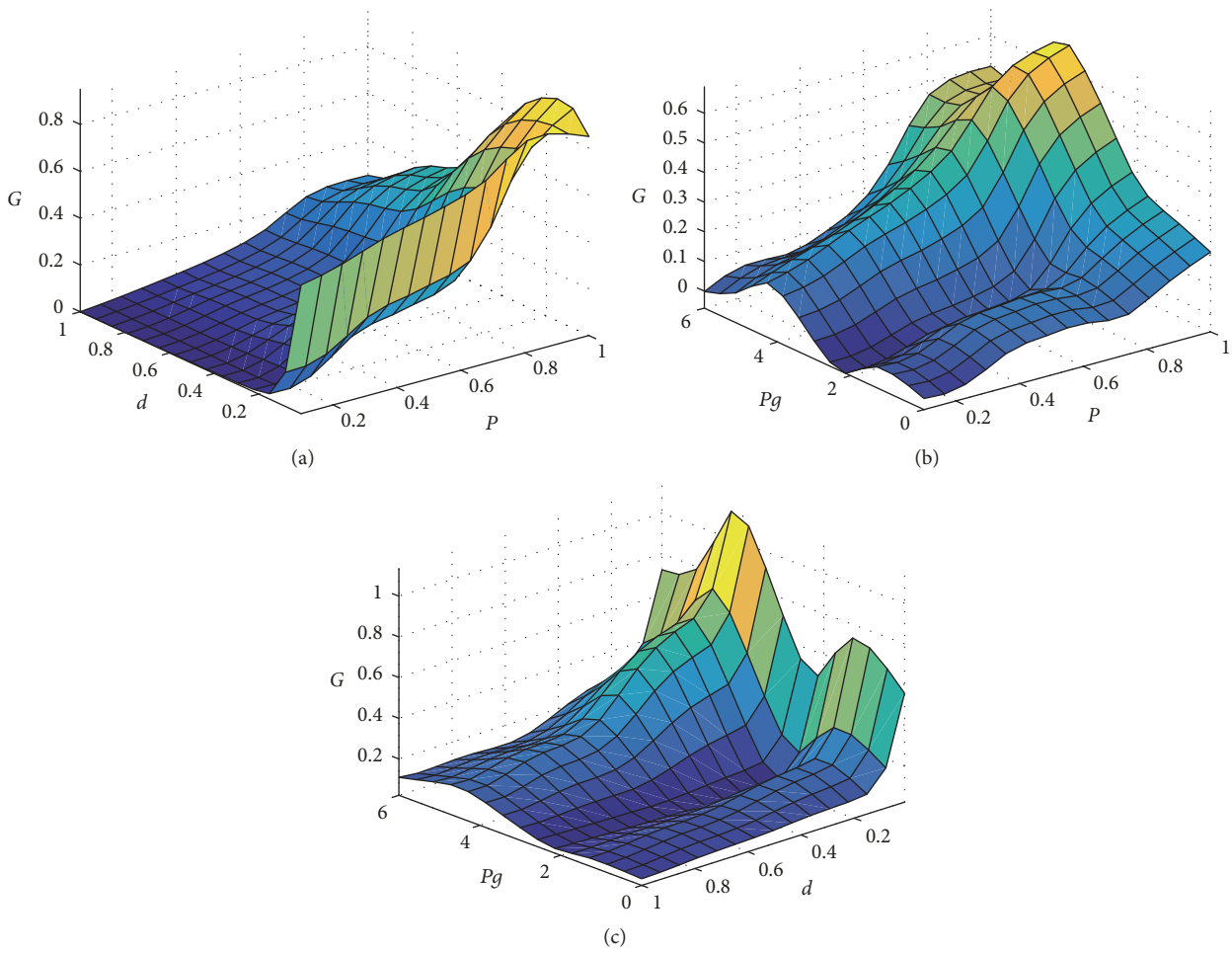


FIGURE 9: ANFIS fuzzy output surfaces:  $P$ - $d$ ,  $P$ - $Pg$ , and  $Pg$ - $d$ , respectively, from (a)–(c).

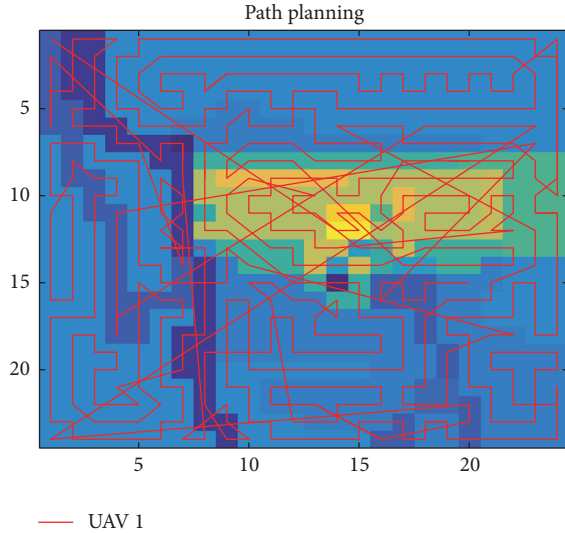


FIGURE 10: La Palma ANFIS path planning.

when scaled to the  $25 \times 25$  map, some problems raised. In addition, in all the previous solutions, the waypoint calculation was very static, all the cells being tracked from its central point. Despite the assumptions made at the beginning regarding this way of tracking each cell, with this PSO solution, we try to find a continuous strategy.

The approach is quite different. We start from the same  $P$  map ( $24 \times 24$  cells), but every cell is divided by 10 to obtain a better discretization. Each new smaller cell has the same  $P$  value than the bigger cell that contains it. Once the map is so divided, the waypoints are searched applying the PSO algorithm.

The variables of the PSO fitness function are the coordinates of the waypoints. The calculation is structured in groups of 10 waypoints, so there will be 20 variables: 10 “ $x$ ” coordinates and 10 “ $y$ ” coordinates. Then, the distance, the weight, and the number of tracked cells are calculated. It is clear that the distance has to be minimized, and the tracked cells need to be maximized, what implies that the UAV is travelling over the maximum number of new cells, since the tracked ones will not be taken into account more than once.

To obtain the tracked cells, a straight path will be traced between two consecutive waypoints, and all the cells inside a square of  $10 \times 10$  along the trajectory will be considered as tracked. That means that the UAV is continually taking images using the same area as in previous solutions. This is the first relevant modification.

Another important modification is that in this case the weight will be maximized. In the previous approaches, a minimization of the weight was interesting because it meant that the UAV first went to the areas with high  $P$  cells. However, with this approach, it is more interesting the opposite because, as said, the calculation is made in bunches of ten waypoints. So, if the weight is maximized for the first ten points, the weight of the second ten points will be lower. That is, the UAV is going over the high  $P$  cells first.

TABLE 6: PSO configuration parameters.

Creation distribution	Uniform
Maximum iterations	4000
Stall Iterations limit	20
Average relative change limit (TolFun)	$10^{-6}$
Swarm size	100
Inertia range	[0.1, 1.1]

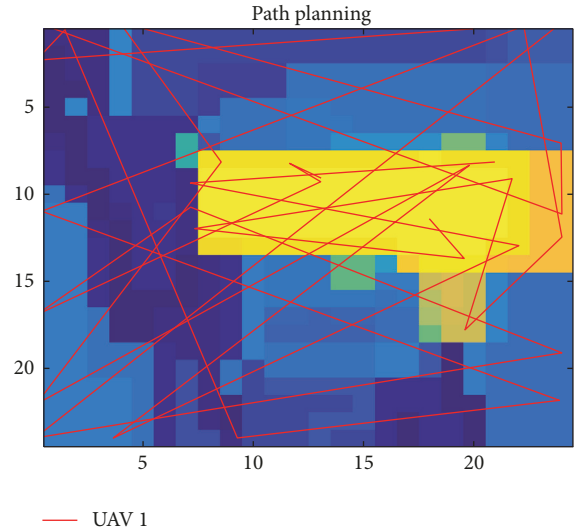


FIGURE 11: La Palma PSO path planning.

The relation between these factors is shown in the following:

$$f = \frac{1}{\left(\sum_{i=1}^{\max(i)} \sum_{j=1}^{\max(j)} \text{covered}(i, j)\right)^{0.1}} + \frac{1}{w^{0.1}} + \left[1 - \frac{1}{d}\right]. \quad (7)$$

The rest of the configuration of the PSO algorithm is shown in Table 6.

Once the setup is finished, the PSO algorithm is applied. The trajectory is shown in Figure 11.

The values of  $d$  and  $w$  are not now calculated because they are not relevant since the nature of the approach is totally different from the previous solutions. But it is worth seeing (Figure 11) how the trajectory has many straight lines covering all the possible space, especially between high  $P$  areas. Many more iterations could have been performed in order to cover the 100% of the map. However, we can also notice that the UAV goes forward and backwards to the same points, which means that this is not such an optimal solution.

## 5. Multiple UAVs Approach

In SAR operations, more than one UAV is usually used. Swarm systems take advantage of simple local behaviours to collectively solve complex problems, where the capability of the group is greater than the sum of its parts [24, 25]. In this

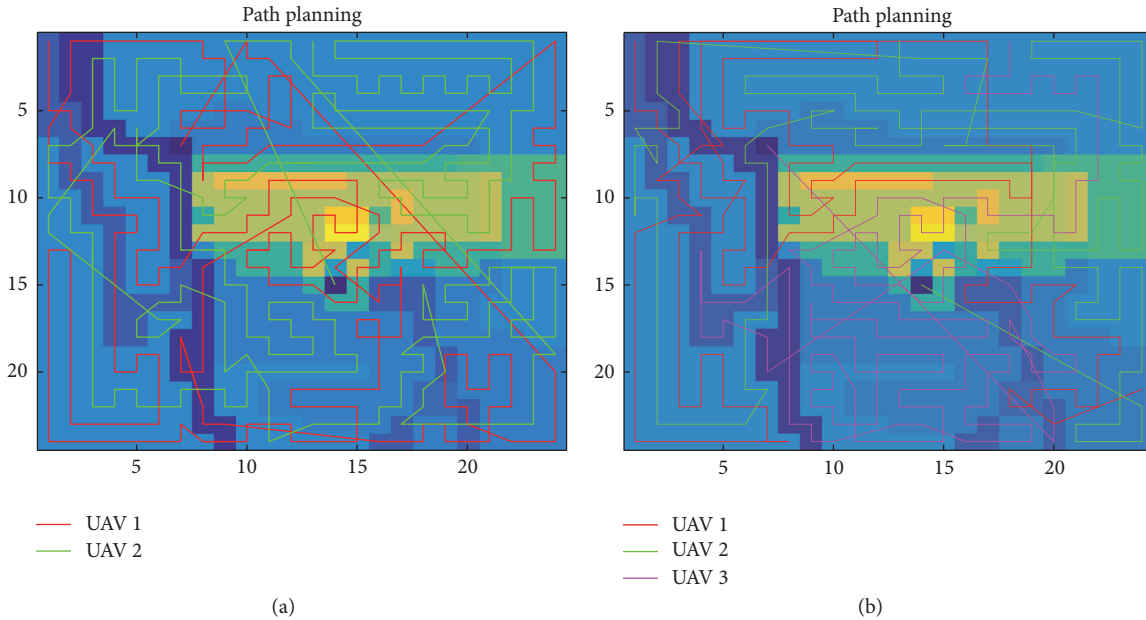


FIGURE 12: La Palma attraction path planning with 2 UAVs (a) and 3 UAVs (b), free formation.

work, two different swarm formations of UAVs for discrete path planning are studied: free and distributed. The UAVs are identical but start from different positions at the map and among them they track all the desired area.

The discrete path planning for several UAVs has been obtained by the attraction, fuzzy logic, and ANFIS approaches. The strategy is the same as the ones presented before for one UAV but now, for every iteration, the number of waypoints calculated is the same as the number of available vehicles. For simplicity, only 1, 2, or 3 UAVs are considered, but the solution could be extended to as many as needed.

In the gridding map of La Palma, the starting point for a 2-UAV configuration is (13, 1) and (18, 1) for 3 UAVs.

**5.1. Free Formation.** Free swarm formation consists of running the path planning algorithm for two or more UAVs at the same time in parallel; that is, each UAV follows an independent path along the coverage area. When calculating new waypoints, the information about the cells tracked by other UAVs is supposedly available, so the rest of the UAVs do not have to visit any already tracked cell.

As an example, Figure 12 shows the trajectories for 2 and 3 UAVs (a and b, resp.), when the attraction approach is used to obtain the discrete path planning.

The results obtained with the attraction path planning approach are  $d = 680$ ,  $w = 37393$  for 1 UAV;  $d = 713$ ,  $w = 19638$  for 2 UAVs; and  $d = 720$ ,  $w = 12812$  for 3 UAVs in free formation. The distance is quite similar in all the cases, but the weight is much lower with more than one UAV.

This effect on the weight is due to the parallel searching. As explained for a single UAV, the weight is calculated multiplying the order each cell is tracked by its  $P$  value, and getting the sum for all cells. In this case, there are two cells

with order 1, two with order 2 and so on, until the UAVs reach half of the number of cells.

The searching time is supposed to be reduced because although the distance is similar, it is shared by several UAVs, so the maximum distance travelled is now about a half or even a third of the distance travelled by only one UAV.

Regarding the path, it is interesting to see how the two UAVs (Figure 12(a)) converge to the green area in the middle of the map at the beginning. Then they separate each other and search in different high  $P$  value areas. At the end, they converge again in low  $P$  value areas. With 3 UAVs, the convergence is not as evident as in this case, meaning a more distributed tracking of every zone.

In all the cases, the trajectories of the different UAVs cross each other. This does not mean collision because the UAVs are not at the same point at the same time. However, the path planning must be completed with a collision avoidance algorithm, which is out of the scope of this work.

The free formation cannot be implemented with the PSO approach due to the nature of the solution, as explained before. For the ANFIS approach, the results are similar, the worst case being the fuzzy one.

**5.2. Distributed Swarm Formation.** A distributed swarm formation of UAVs means that the map is divided into several parts, as many as vehicles, and each UAV is assigned an area which it must track.

The path planning for 2 and 3 UAVs in a distributed swarm formation with the attraction path planning is shown in Figure 13. It is possible to see how each UAV tracks an independent zone and their paths do not cross. The distances are now  $d = 673$  for 2 UAVs and  $d = 678$  for 3 UAVs, and the weights  $w = 20411$  and  $w = 13712$ , respectively. The distance

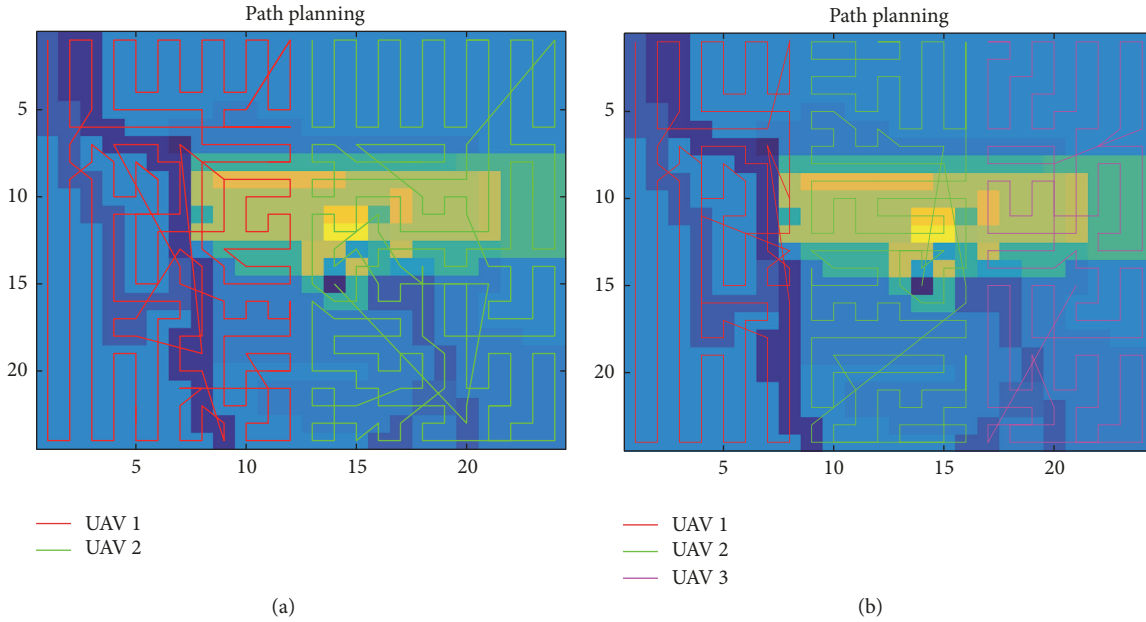


FIGURE 13: La Palma attraction path planning with 2 UAVs (a) and 3 UAVs (b), distributed formation.

TABLE 7: Comparison between the different approaches.

Formation	1 UAV		2 UAV				3 UAV			
	$w$	$d$	Free		Distributed		Free		Distributed	
	$w$	$d$	$w$	$d$	$w$	$d$	$w$	$d$	$w$	$d$
Attraction	37393	680	19638	713	20411	673	12812	720	13712	678
Fuzzy logic	35951	1497	17931	1550	19219	1212	12137	1596	13119	1155
ANFIS	36284	808	18579	827	19474	716	12520	876	13386	732

is similar but slightly longer than with only one UAV (680) and slightly better than the travelled distance obtained with UAVs in free formation (713 and 720). Regarding the weight, it is much smaller than the case of one UAV (37392) and much better for 3 UAVs than with 2 UAVs.

The same experiments have been carried out with different number of UAVs for the different approaches proposed (fuzzy logic and ANFIS).

*5.3. Comparison of the Approaches with Different Number of UAVs.* Finally, Table 7 summarizes the results of the different approaches for the two configurations. As expected, the results improve when the number of UAVs is increased. This is mainly due to the way the weight is calculated and proves the validity of the proposed strategies.

In general terms, it can be seen how the different methods have strong and weak points. The attraction method is the one with shortest paths, followed by the ANFIS one. However its weights are slightly higher than the other methods. Indeed, the fuzzy logic one has the lowest weight values although the difference is not big, but with much longer distances than the other two methods. In that sense, the ANFIS method has the most balanced results, with medium weights and low distance values.

To summarize, it is difficult to say which is better. It depends on the priority of the goals. The quickest is the attraction strategy, but the fuzzy approach is the best one finding people, at least visiting the areas where it is most probable to find someone. We will check these results on a real case in the next section.

## 6. A Case Studied

To analyze and prove the validity and utility of the discrete path planning proposals presented in this paper, they are going to be compared on a SAR real scenario.

Thirty missing people have been randomly located on the potential risk/occupancy map of La Palma. A uniformly distributed random generator gives a value that is associated with each cell of the map. Then, this value is multiplied by half of the potential risk/occupancy value of that cell. The resulting 25 positions with the highest value are selected. In this way we obtain a random distribution but weighted towards areas with high  $P$  values. The remaining 5 cases are manually distributed on areas with low  $P$  values (Figure 14). These last ones are set as the first five cases to be found so that they can be easily located in the graphs showing the time results of the searching.

TABLE 8: Time results with attraction strategy.

	1 UAV	2 UAVs		3 UAVs	
		Free	Distributed	Free	Distributed
Mean	217.62	113.88	115.60	88.84	87.60
Wins	1.00	2.00	2.00	3.00	1.00
Losses	6.00	0.00	5.00	0.00	0.00
Total wins			9.00		
Total losses			11.00		

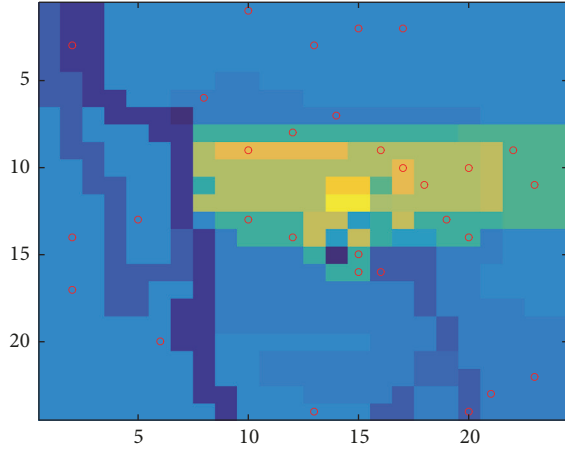


FIGURE 14: La Palma missing people.

The main criterion used to test the strategies is the time the UAV needs to find each of the 30 people individually. It is supposed to be proportional to the distance. All the UAVs are considered to have the same technical characteristics and to fly at the same speed (set to 3). Another assumption has been considered to make the simulation more realistic. When the UAV is tracking a cell, its speed is lower than when it is moving between different areas (tracking speed = 1).

Each case (finding someone) is evaluated estimating the time it takes the UAV to get there from the initial position with a particular configuration (strategy and formation).

When the cases are evaluated, the time that each method and its training require is calculated. For each case there is a method with a particular formation that has been the fastest, it is a winner; and there has been another one that has been the slowest, that is, a loose one. There should be a total of 30 wins and 30 losses adding all the possible configurations and strategies results, but there are some more because since the space and the speed are discretized, in some cases, there are ties.

In this way, we can compare the different methods, to see which are the best one exploring low  $P$  zones or high  $P$  cells and so on.

**6.1. Finding People with the Attraction Strategy.** The time results for attraction path planning are shown in Table 8. The number of wins represents the number of times that a specific configuration was the best one among the others. The number of losses represents when it was the worst one.

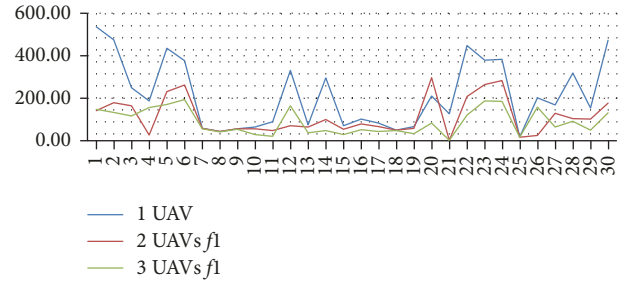


FIGURE 15: La Palma attraction path planning results for free swarm.

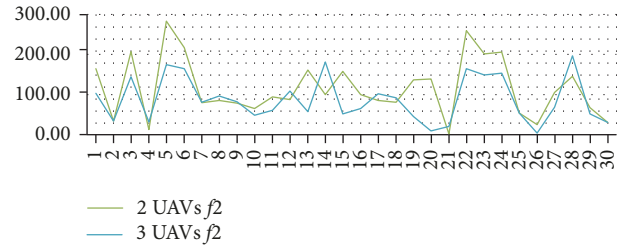


FIGURE 16: La Palma attraction path planning results for distributed swarm.

Figures 15 and 16 show the comparison between different number of UAV for this strategy. Time unit is represented in the vertical axis and the case in the horizontal one.

As expected, the time is reduced when the number of UAVs increases. Besides, the first five points need more time because they have low  $P$  values, so the UAV goes there after going to the higher  $P$  ones.

A comparison between the two swarm configurations with the same number of UAVs is shown in Figure 17 (free,  $f1$ ; distributed,  $f2$ ). We can observe that with two UAVs the difference is not significant. Nevertheless, with three UAVs, even having a similar tendency, there are big differences in some of the cases, which indicates that the searching is done with a very different philosophy.

**6.2. Fuzzy Logic Path Planning.** The results obtained with the fuzzy logic path planning are shown in Table 9.

In this case, there are more winning configurations. The worst ones are almost exclusively associated with the use of only one UAV. That means that this method is inefficient for one UAV, but its efficiency is highly improved when

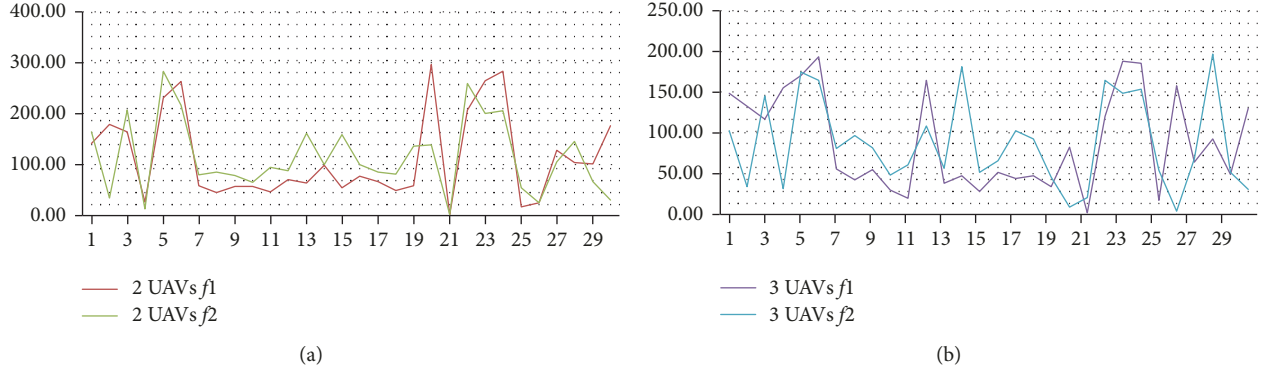


FIGURE 17: La Palma attraction path planning results for 2 UAVs (a) and 3 UAVs (b).

TABLE 9: Time results with fuzzy logic path planning.

	1 UAV	2 UAVs		3 UAVs	
		Free	Distributed	Free	Distributed
Mean	257.90	120.02	109.71	84.95	59.05
Wins	0.00	0.00	2.00	3.00	9.00
Losses	11.00	0.00	1.00	0.00	0.00
Total wins			14.00		
Total losses			12.00		

TABLE 10: Time results with ANFIS path planning.

	1 UAV	2 UAVs		3 UAVs	
		Free	Distributed	Free	Distributed
Mean	212.70	117.33	107.94	74.99	86.23
Wins	0.00	3.00	2.00	8.00	3.00
Losses	8.00	0.00	0.00	0.00	0.00
Total wins			16.00		
Total losses			8.00		

increasing the number of UAVs, especially in distributed formation.

**6.3. ANFIS Path Planning Results.** The results obtained for the ANFIS path planning are shown in Table 10.

Although this method seems to be the best one in terms of finding people, it has the same problem as the fuzzy logic approach. That is, better results are obtained with free swarm formation than with the distributed one; the worst case is again with an only UAV. Anyway, this strategy gives the best average values for this scenario.

**6.4. PSO Path Planning Results in a SAR Mission.** PSO path planning obtains the worst results of all. This method does not work well because the UAV travels long distances between waypoints in order to cover the surface with a distance/speed relation of one. Due to the continuous tracking, the UAV is very slow in comparison to the other methods. All results obtained are worse than with the other solutions, with many losses, meaning that the UAV did not find that people (Figure 18).

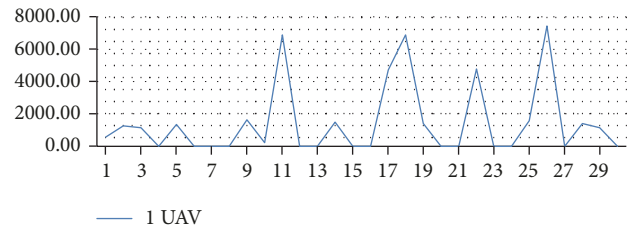


FIGURE 18: La Palma PSO path planning results.

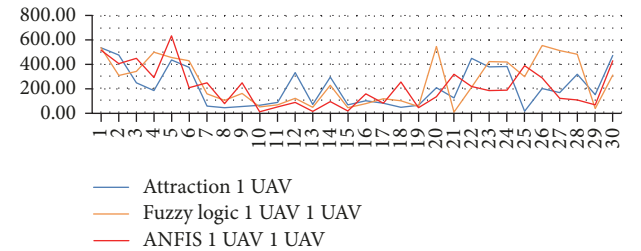


FIGURE 19: La Palma path planning results comparison for 1 UAV.

In view of these results, PSO is not taken into account for the global comparison between the different methods.

## 7. Discussion of the Global Results

A comparison between the different methods and configurations is carried out and the global results are discussed. To have a good overview, every strategy has been applied to the same 30 cases, with the two possible formations when more than one UAV is used in the searching.

First, Figure 19 shows the three different searching strategies with one UAV. The time results are very similar but, in general, ANFIS path planning is slightly better. The three methods work well with low  $P$  cells, but attraction gets shorter time than the others finding those worse cases.

In Figures 20 and 21, the path planning results for two and three UAVs, respectively, in free swarm formation are shown. Results are again quite similar. Fuzzy logic path planning seems to be somewhat worse than the others.

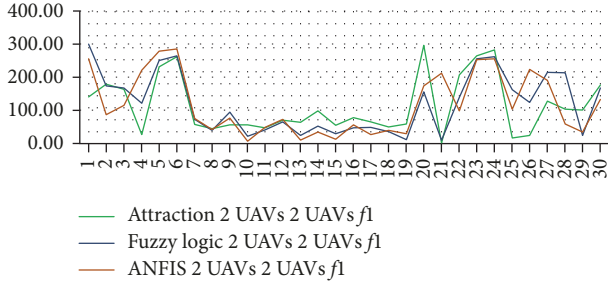


FIGURE 20: La Palma results comparison for 2 UAVs in free formation.

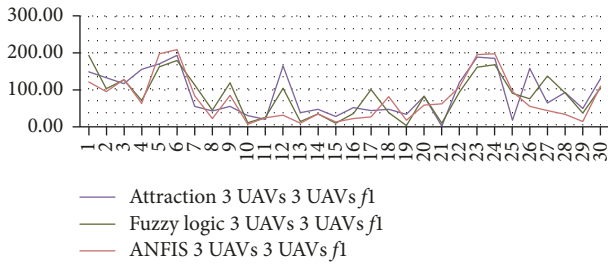


FIGURE 21: La Palma results comparison for 3 UAVs in free formation.

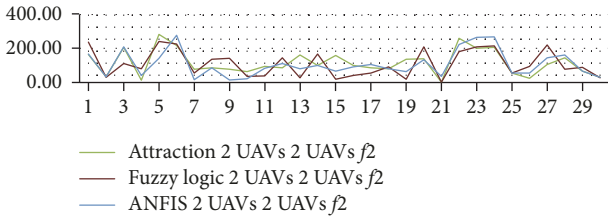


FIGURE 22: La Palma results comparison for 2 UAVs in distributed formation.

For distributed swarm configuration, Figures 22 and 23 show the results for 2 and 3 UAVs, respectively. The results for 2 UAVs are once again similar for all methods, having the ANFIS approach a slightly better performance.

However, in Figure 23, it is possible to see that there is a big difference between the fuzzy logic approach and the others. This method works better in distributed swarm maybe because it was designed for smaller maps, so when the searching area is smaller, the performance of this approach improves.

Finally, Figure 24 shows the average time of each configuration for every approach. According to these results, the fastest configuration for searching is to have 3 UAVs in distributed swarm formation ( $f2$ ), as expected, and fuzzy logic approach gives the best results for this particular configuration, having ANFIS and attraction similar searching time.

Nevertheless, regarding the number of losses and wins (Figure 25), which is a critical factor, the ANFIS method is in general the best one. The fuzzy logic has also a very good

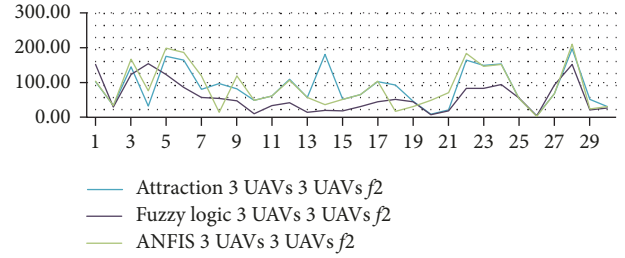


FIGURE 23: La Palma results comparison for 3 UAVs in distributed formation.

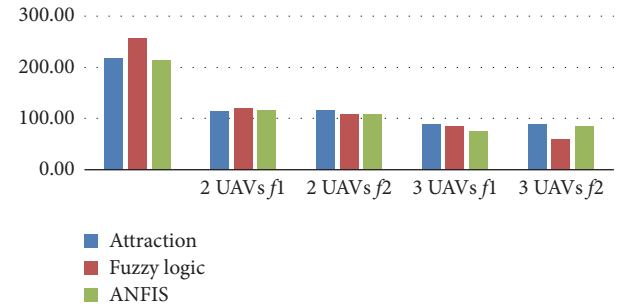


FIGURE 24: La Palma path planning mean time for all the configurations and every approach.

performance, especially for distributed configurations, as it has been said. However, even having less number of wins, attraction method is the most consistent due to its small number of losses, which indicates that its results are quite balanced.

As a summary, we can say that the attraction method gets medium positions regarding efficiency. It performs a regular and extensive search, which implies that it does not take it a lot of time finding people in low  $P$  areas, but it does not go as fast as other methods to high  $P$  values zones. This method works very well for homogenous  $P$  maps.

Fuzzy logic presents a quite fast convergence but it is very irregular. However, it works well in maps with large high  $P$  areas due to its type of searching, which performs like a random search in all dangerous areas.

The ANFIS approach has been proven to be the best one in general terms. It has a fast convergence to high  $P$  values and also performs a quite regular searching on the rest of the cells. It works worse on low  $P$  areas that are far from high  $P$  ones, where other methods have obtained better results.

## 8. Conclusions and Future Work

In this work, two main contributions are presented. The first one is a fuzzy map generation of a searching area according to a risk/occupancy factor that aims at search and rescue (SAR) missions. The second one is the application of different intelligent strategies for discrete path planning to cover a gridding searching area.

Regarding the map characterization, the conclusion is that it helps to focus the path planning on promising zones.

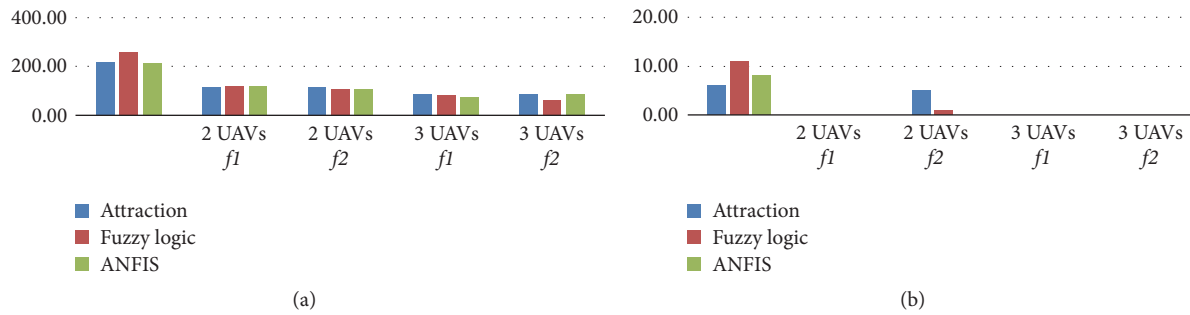


FIGURE 25: La Palma wins (a) and losses (b) cases.

The path planner finds trajectories that minimize the risk the people are exposed to. Indeed, in the simulations results, a fast tracking of the higher probability risk/occupied areas can be observed that results in a quicker finding of the people involved in a dangerous situation.

Four intelligent strategies have been applied to the discrete path planning, namely, attraction, an original one, and fuzzy, ANFIS, and PSO. Except this last one, the rest have obtained good results in terms of searching time and distance. Another conclusion is that the performance of the method strongly depends on the associated probability map. This remarks the importance of the generation of this map, taking into account all the possible variables and factors that can influence the searching.

Using multiple UAVs in swarm formation for the searching, a dependence on the type of path planning method has been observed. In general, distributed formation works better, but it should be chosen in association with the  $P$  map and the path planning method.

Future works related to several aspects of this work could be the following:

- (i) Studying other factors for the map characterization and their influence on the potential risk/occupancy value, which has been proved important for the SAR mission
- (ii) Working with a more realistic model of the UAVs, including the dynamics [26], and also avoidance and visual tracking algorithms [27]
- (iii) Testing the most successful proposals on real systems.

## Conflicts of Interest

The authors declare that there are no conflicts of interest regarding the publication of this article.

## Acknowledgments

This work is supported by the European Union EP-INTERREG V-A Spain-Portugal (POCTEP), Project 0115\_TECNOLIVO\_6\_E, which provided funds for covering the costs to publish the paper in open access.

## References

- [1] L. Novaro Mascarello and F. Quagliotti, "The civil use of small unmanned aerial systems (sUASs): operational and safety challenges," *Aircraft Engineering and Aerospace Technology*, vol. 89, no. 5, pp. 703–708, 2017.
- [2] G. Pajares, J. J. Ruz, P. Lanillos, M. Guijarro, J. M. De La Cruz, and M. Santos, "Trajectory generation and decision making for UAVs," *RIAI - Revista Iberoamericana de Automatica e Informatica Industrial*, vol. 5, no. 1, pp. 83–92, 2008.
- [3] P. García-Auñón, M. Santos-Peñas, and J. M. de la Cruz García, "Parameter selection based on fuzzy logic to improve UAV path-following algorithms," *Journal of Applied Logic*, vol. 24, no. part B, pp. 62–75, 2017.
- [4] M. Silvagni, A. Tonoli, E. Zenerino, and M. Chiaberge, "Multipurpose UAV for search and rescue operations in mountain avalanche events," *Geomatics, Natural Hazards and Risk*, vol. 8, no. 1, pp. 18–33, 2017.
- [5] R. Dubé, A. Gawel, C. Cadena, R. Siegwart, L. Freda, and M. Gianni, "3D localization, mapping and path planning for search and rescue operations," in *Proceedings of the 14th International Symposium on Safety, Security and Rescue Robotics, SSRR 2016*, pp. 272–273, Switzerland, October 2016.
- [6] M. Jun and R. D'Andrea, "Path Planning for Unmanned Aerial Vehicles in Uncertain and Adversarial Environments," in *Cooperative Control: Models, Applications and Algorithms*, vol. 1 of *Cooperative Systems*, pp. 95–110, Springer US, Boston, MA, 2003.
- [7] F. Kamrani and R. Ayani, *UAV path planning in search operations*, Aerial Vehicles, InTech, 2009.
- [8] C. Baker, G. Ramchurn, L. Teacy, and N. Jennings, "Planning search and rescue missions for UAV teams," in *Proceedings of the At 2016: Conference on Prestigious Applications of Intelligent Systems at ECAI, 2016*, p. 6, 2016.
- [9] K. P. Valavanis and G. J. Vachtsevanos, "Uav mission and path planning: Introduction," *Handbook of Unmanned Aerial Vehicles*, pp. 1443–1446, 2015.
- [10] E. Besada-Portas, L. de La Torre, J. M. de La Cruz, and B. de Andrés-Toro, "Evolutionary trajectory planner for multiple UAVs in realistic scenarios," *IEEE Transactions on Robotics*, vol. 26, no. 4, pp. 619–634, 2010.
- [11] M. D. Phung, C. H. Quach, T. H. Dinh, and Q. Ha, "Enhanced discrete particle swarm optimization path planning for UAV vision-based surface inspection," *Automation in Construction*, vol. 81, pp. 25–33, 2017.

- [12] G. E. Anaya Fuentes, E. S. Hernández Gress, J. C. Seck Tuoh Mora, and J. Medina Marín, "Solution of the job-shop scheduling problem through the traveling salesman problem," *RIAI - Revista Iberoamericana de Automatica e Informatica Industrial*, vol. 13, no. 4, pp. 430–437, 2016.
- [13] M. Kallmann and M. Kapadia, "Geometric and Discrete Path Planning for Interactive Virtual Worlds," *Synthesis Lectures on Visual Computing*, vol. 8, no. 1, pp. 1–201, 2016.
- [14] P. B. Sujit, S. Saripalli, and J. B. Sousa, "An evaluation of UAV path following algorithms," in *Proceedings of the 2013 12th European Control Conference, ECC 2013*, pp. 3332–3337, che, July 2013.
- [15] A. Barrientos, P. Gutiérrez, and J. Colorado, *Advanced UAV trajectory generation: Planning and guidance*, Aerial Vehicles, InTech, 2009.
- [16] E. G. Hernandez-Martinez, E. D. Ferreira-Vazquez, G. Fernandez-Anaya, and J. J. Flores-Godoy, "Formation tracking of heterogeneous mobile agents using distance and area constraints," *Complexity*, vol. 2017, Article ID 9404193, 2017.
- [17] E. Besada-Portas, L. De La Torre, A. Moreno, and J. L. Risco-Martín, "On the performance comparison of multi-objective evolutionary UAV path planners," *Information Sciences*, vol. 238, pp. 111–125, 2013.
- [18] P. García Auñón and M. Santos, "Use of genetic algorithms for unmanned aerial systems path planning in. Decision Making and Soft Computing," *World Scientific*, vol. 9, pp. 430–435, 2014.
- [19] M. Davoodi, F. Panahi, A. Mohades, and S. N. Hashemi, "Multi-objective path planning in discrete space," *Applied Soft Computing*, vol. 13, no. 1, pp. 709–720, 2013.
- [20] F. Alonso Zotes and M. Santos Peñas, "Heuristic Optimization of Interplanetary Trajectories in Aerospace Missions," *RIAI - Revista Iberoamericana de Automatica e Informatica Industrial*, vol. 14, no. 1, pp. 1–15, 2017.
- [21] P. Yang, K. Tang, and J. A. Lozano, "Estimation of Distribution Algorithms based Unmanned Aerial Vehicle path planner using a new coordinate system," in *Proceedings of the 2014 IEEE Congress on Evolutionary Computation, CEC 2014*, pp. 1469–1476, China, July 2014.
- [22] -J. Ruz, O. Arévalo, G. Pajares, and M. J. De Cruz, *UAV trajectory planning for static and dynamic environments*, Aerial Vehicles, InTech, 2009.
- [23] J. S. R. Jang, "ANFIS: adaptive-network-based fuzzy inference system," *IEEE Transactions on Systems, Man, and Cybernetics*, vol. 23, no. 3, pp. 665–685, 1993.
- [24] T. Tomic, K. Schmid, P. Lutz et al., "Toward a fully autonomous UAV: research platform for indoor and outdoor urban search and rescue," *IEEE Robotics and Automation Magazine*, vol. 19, no. 3, pp. 46–56, 2012.
- [25] J. B. Seco, J. Dormido Canto, M. Montalvo Martinez, J. López-Orozco, E. Besada Portas, and J. De la Cruz García, "Centro de Control de Tierra para Colaboración de Vehículos Autónomos Marinos," *Revista Iberoamericana de Automática e Informática industrial*, vol. 15, no. 1, p. 1, 2017.
- [26] J. E. Sierra and M. Santos, "Modelling engineering systems using analytical and neural techniques: Hybridization," *Neurocomputing*, 2017.
- [27] Z. Wu, Z. Guan, C. Yang, and J. Li, "Terminal guidance law for UAV based on receding horizon control strategy," *Complexity*, vol. 2017, pp. 1–19, 2017.

